Sensors & Actuators: B. Chemical 392 (2023) 134048

Contents lists available at ScienceDirect

Sensors and Actuators: B. Chemical

journal homepage: www.elsevier.com/locate/snb

Sensitivity–Enhanced detection of acetone gas using MXene-Immobilized planar microwave sensor

Luqman Ali [a,1], Jie Wei [a,1], Fan-Yi Meng [a], Muhammad Waqas Qureshi [b], Kishor Kumar Adhikari [a,g,*], Ming-Yu Li [c], Jun-Ge Liang [d], Xiao-Long Wang [e], Xu-Min Ding [a], Nam-Young Kim [f,**], Cong Wang [a,**]

[a] School of Electronics and Information Engineering, Harbin Institute of Technology, Harbin 150001, China
[b] Department of Material Science and Engineering, University of Wisconsin, Madison, WI 53706, USA
[c] School of Science, Wuhan University of Technology, Wuhan 430070, China
[d] Department of Electronic Engineering, Jiangnan University, Jiangsu, China
[e] College of Electronic Science and Engineering, Jilin University, China
[f] Department of Electronic Engineering, Kwangwoon University, Seoul 139-701, Republic of Korea
[g] Department of Electronics and Computer Engineering, National College of Engineering, Tribhuvan University, Lalitpur 44700, Nepal

ARTICLE INFO

Keywords:
Acetone gas
Enhanced sensitivity
Gas sensor
MXene
Noncontact immobilization
Planar microwave resonator

ABSTRACT

This work presents the noncontact immobilization of $Ti_3C_2T_x$ MXene on a planar microwave resonator sensor via a polyimide film to enhance the gas detection sensitivity, enabling the characterization of the part per million-level of acetone gas. Sandwiching a polyimide (PI) film confined an intense electromagnetic field between the resonator's interdigital capacitor structure and the MXene layer, maintaining a significant interaction between the acetone gas molecules and the resonator's EM field via the MXene layer. Therefore, contactless immobilization of the MXene layer enhanced the acetone gas detection sensitivity by 110% compared to the resonator gas sensor with MXene deposited directly on the resonator surface. As a proof of concept, two sensor prototypes were implemented using resonators with layers of PI film and MXene and resonators with MXene only and were applied to detect a wide range of acetone gas concentrations. Immobilizing the layers of PI film and MXene on the microwave resonator achieved a linear correlation between the resonant frequency and acetone gas concentration with high sensitivity (17.85 kHz/ppm, a fast response time (60 s), and recovery time (85 s).

1. Introduction

Detection and characterization of gases based on their electrical properties (relative permittivity and conductivity) using microwave-based sensors have captured growing attention, mainly because of their room temperature operation and multi-parameter detection [1–3]. In addition, their applicability in harsh and hazardous environments enabled by the wireless and contactless operation has rendered them the gas sensing technology of incremental interest for numerous potential applications, such as personalized exposure assessment for safety in industries, food quality monitoring, and environmental quality control [4–10]. Among different types of microwave gas sensors, planar microwave resonator-based gas sensors are more attractive due to their low cost, ease of implementation, small footprint, and robustness [11–13]. However, the sensitivity of planar microwave resonator-based gas sensors is an essential parameter that still poses significant challenges in using these gas sensors for monitoring low-concentration gases, including volatile organic compounds (VOCs). Some applications that require detecting low concentrations of VOCs, for example, include detecting acetone gas for diabetes monitoring [14] and analyzing heart failure severity [15].

Planar microwave resonator gas sensors consist of engineered geometries of metal microstrip lines on a dielectric substrate and a gas-sensitive material as the interface to target a specific gas. Following the method mentioned, Rydosz et al. investigated the potential of an interdigital capacitor-based microwave resonator sensor immobilized

* Corresponding author at: School of Electronics and Information Engineering, Harbin Institute of Technology, Harbin 150001, China.
** Corresponding authors.
E-mail addresses: kishordhkr@live.com (K.K. Adhikari), nykim@kw.ac.kr (N.-Y. Kim), kevinwang@jit.edu.cn (C. Wang).
[1] Luqman Ali and Jie Wei contributed equally to this work.

https://doi.org/10.1016/j.snb.2023.134048
Received 3 April 2023; Received in revised form 22 May 2023; Accepted 29 May 2023
Available online 30 May 2023

with comb copolymer phthalocyanine (Pc) to detect different VOCs (acetone, ethanol, and methanol) [16]. The presented sensor could detect acetone ranging from 5 ppm to 200 ppm using the shift in resonant frequency at room temperature. Integrating a planar microwave resonator with the nanocomposite of graphene oxide (GO)-polyaniline (PANI), Javadian-Saraf et al. developed an ammonia gas sensor. Using this method, ammonia gas, ranging from 1 ppm to 250 ppm, was detected with a response time of 150 s and sensitivity of up to 0.03 dB/ppm, exploiting the change in the sensor's resonant amplitude [17]. Among various resonator configurations, electric inductor-capacitor (ELC) resonators are amongst the most widely investigated resonator structures to implement microwave sensors with a simple layout, small footprint, and moderate sensitivity for detecting and characterizing materials in solid, liquid, and gas phases [18–23]. Yu et al. developed a humidity sensor by immobilizing a microfabricated LC resonator on gallium arsenide with carbon dot-decorated porous Co_3O_4 [24]. Using a thin layer of polydimethylsiloxane (PDMS) layer as an interface, Zarifi et al. demonstrated the potential of a split-ring resonator (SRR) sensor, equivalently an ELC resonator, to detect acetone gas [25]. Gas absorption-based swelling and change in permittivity of the PDMS layer enabled the developed sensor to detect acetone gas with a concentration ranging from 0% to 26.5% using the shift in resonant frequency. A differential sensor consisting of PDMS-coated SRR in a power splitter/-combiner configuration was introduced by Mohammadi et al. to detect VOC gases, including acetone (387–31024 ppm), ethanol, methanol, and isopropyl alcohol [26]. Thus, the literature review shows the continuous efforts toward implementing microwave resonator gas sensors for the sensitive detection of acetone gas. However, detecting and distinguishing low-concentration acetone gas is still challenging, urging the development of a microwave resonator gas sensor featuring high sensitivity to enhance the frontier of microwave detection in monitoring low-concentration acetone gas for various applications.

MXene, a growing family of two-dimensional (2D) materials, has recently received significant attention from researchers for numerous potential applications, including energy storage [27], electromagnetic interference (EMI) shielding [28], catalysis [29], and biosensors [30]. Among different types of MXenes reported to date, titanium carbide ($Ti_3C_2T_x$) has been most widely investigated, mainly due to its high conductivity (up to 10,000 S cm^{-1}), excellent flexibility, and superior mechanical strength [31,32]. Besides, $Ti_3C_2T_x$ MXene offers the flexibility to terminate its surface with functional groups, such as oxygen (-O), hydroxyl (-OH), and fluorine (-F), which make it a potential candidate for gas sensing applications [33]. In an overview of the recent progress in the synthesis and applications of MXene, Khan et al. reported that MXene has recently gained incremental attention in humidity and gas sensing applications [34]. Based on a chemoresistive gas sensor, Simonenko et al. investigated the gas-sensing characteristics of titanium carbide MXenes, demonstrating their high sensitivity and selective performance [35]. Using $Ti_3C_2T_x$ MXene as an interface material, Lee et al. demonstrated the potential of an interdigital capacitor sensor to detect VOC gases (ethanol, methanol, acetone, and ammonia) at room temperature [36]. In work on a chemiresistive sensor employing $Ti_3C_2T_x$ MXene as a metallic channel, Kim et al. demonstrated the detection of VOC gases as low as 50 parts per billion [37]. Kasra et al. used a $Ti_3C_2T_x$ MXene membrane to develop a 1.834 GHz patch antenna, which was further used as a sensing and radiating element to implement a wireless gas sensor. The MXene antenna sensor could detect acetone gas with a concentration ranging from 0.8% to 8% with a fast response time of 23 s, where the results were monitored wirelessly using another antenna from a distance of 1.5 m [38]. Despite the potential of MXenes in acetone gas sensing shown by previous studies, their feasibility as interface material has not been investigated yet to implement a high-sensitivity microwave-based acetone gas sensor. A challenge associated with MXene as gas-sensitive interface material lies in their high conductivity and electromagnetic (EM) loss, which adversely impacts the quality factor of a microwave resonator; and the resulting sensitivity to detect gas.

This work presents a planar microwave resonator sensor immobilized with MXene for sensitivity-enhanced detection and characterization of acetone gas. MXene was strategically immobilized on the resonator surface via polyimide substrate, minimizing the impact of EM loss of MXene, consequently enhancing the sensitivity to detect acetone gas significantly. The developed MXene-based microwave resonator gas sensor was used to detect a physiologically relevant range of acetone gas concentrations (1–500 ppm).

2. Experimental section

2.1. Materials

Ti_3AlC_2 powder (Shandong Kaiene Ceramics, China), HCl (12 M, Sinopharm, China), and LiF (Aladdin Shanghai, China) of analytical grade were used in this work. In addition, distilled water was used throughout the experiment to synthesize MXene.

2.2. Preparation of multilayer $Ti_3C_2T_x$ MXene

MXene with different terminations was synthesized from MAX phase materials with the chemical formula of Ti_3AlC_2 by minimal intensive layer delamination (MILD). Fig. 1(a) depicts the schematics of $Ti_3C_2T_x$ MXene preparation. The etching solution was typically prepared by dissolving 4 g LiF (Aladdin Shanghai, China) into 45 mL HCl (12 M, Sinopharm, China). Then, 2 g Ti_3AlC_2 powder (Shandong Kaiene Ceramics, China) was slowly added to the etching solution and continuously stirred by magnetons at 45 °C for 24 h. After etching, the precipitate was washed with deionized water until the supernatant showed neutral pH. The prepared multilayer $Ti_3C_2T_x$ was then dispersed in 20% LiCl solution, followed by 4 h of stirring for complete mixing. The mixture was finally centrifuged for 5 min at 3500 rpm until the supernatant turned black for spraying purposes.

2.3. MXene-based microwave gas sensor fabrication and measurement

An ELC resonator structure was used to implement the MXene-based microwave gas sensor. Fig. 2(a) presents the schematic of the proposed ELC resonator where the inductor was implemented using the outer square ring, and the capacitor was patterned using an interdigital structure. Owing to the confinement of an intense EM field, the interdigital capacitor was the core of the proposed resonator sensor, where the MXene layer was deposited as a gas-sensitive interface (See Fig. S1). MXene was functionalized on the resonator's interdigital structure using two approaches, as illustrated in Fig. 2. First, the $Ti_3C_2T_x$ MXene was deposited directly on the interdigital structure of the proposed resonator, as shown in Fig. 2(d) and 2 (e). Initially, the PI tape was used to cover the resonator, exposing only the interdigital structure, where MXene was spray-coated, and the resulting sensor was allowed to dry in a vacuum chamber at room temperature for 12 h. Under similar conditions in the second approach, a PI tape was also placed over the interdigital digital structure, which was followed by the spray coating of Mxene. The sensitivity of the designed sensor with the MXene-PI layer (0.01538 GHz/ε_r) was 1.4 times more sensitive than the sensor with just MXene (0.00281 GHz/ε_r), thereby validating the proposed concept.

Custom-designed stainless steel gas chamber, operable in a static mode, was used to perform gas sensing experiment, evaluating the acetone gas detection characteristics of the developed MXene microwave sensor. The fabricated gas sensor was placed inside the sample holder and connected with a Keysight Technologies vector network analyzer (VNA) (N9916A) to measure the sensor's insertion loss (see Supplementary Fig. S2). Next, the chamber door was sealed, followed by the constant flow of clean air, maintaining an atmospheric pressure. The resonant frequency and amplitude were measured and used as the baseline sensing parameters. The microwave gas sensing system was used in a static mode, where a gas sample was confined within a sealed

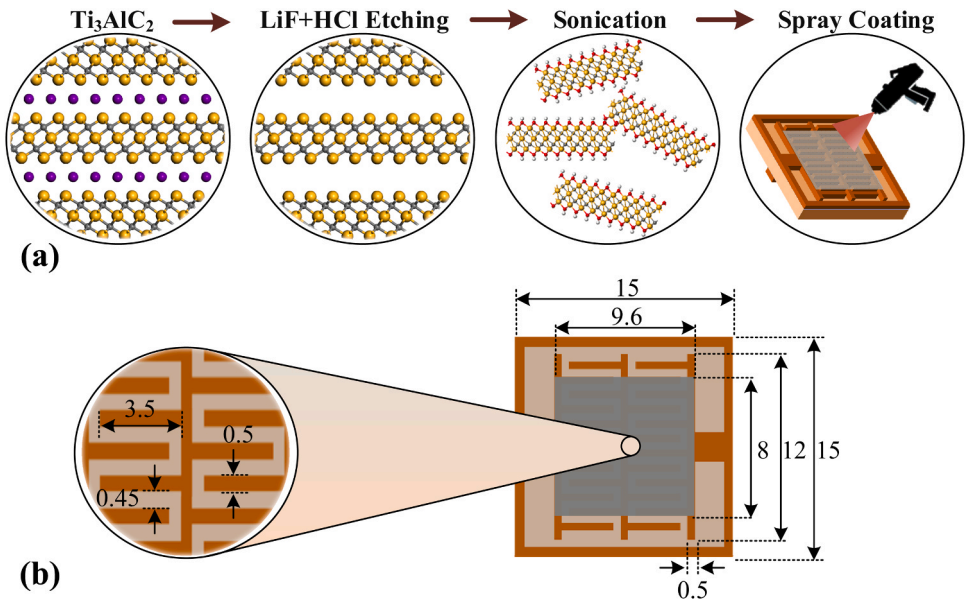

Fig. 1. (a) Synthesis of $Ti_3C_2T_x$ MXene and its deposition on the resonator surface using spray coating and (b) dimensions of the proposed microwave sensor in mm.

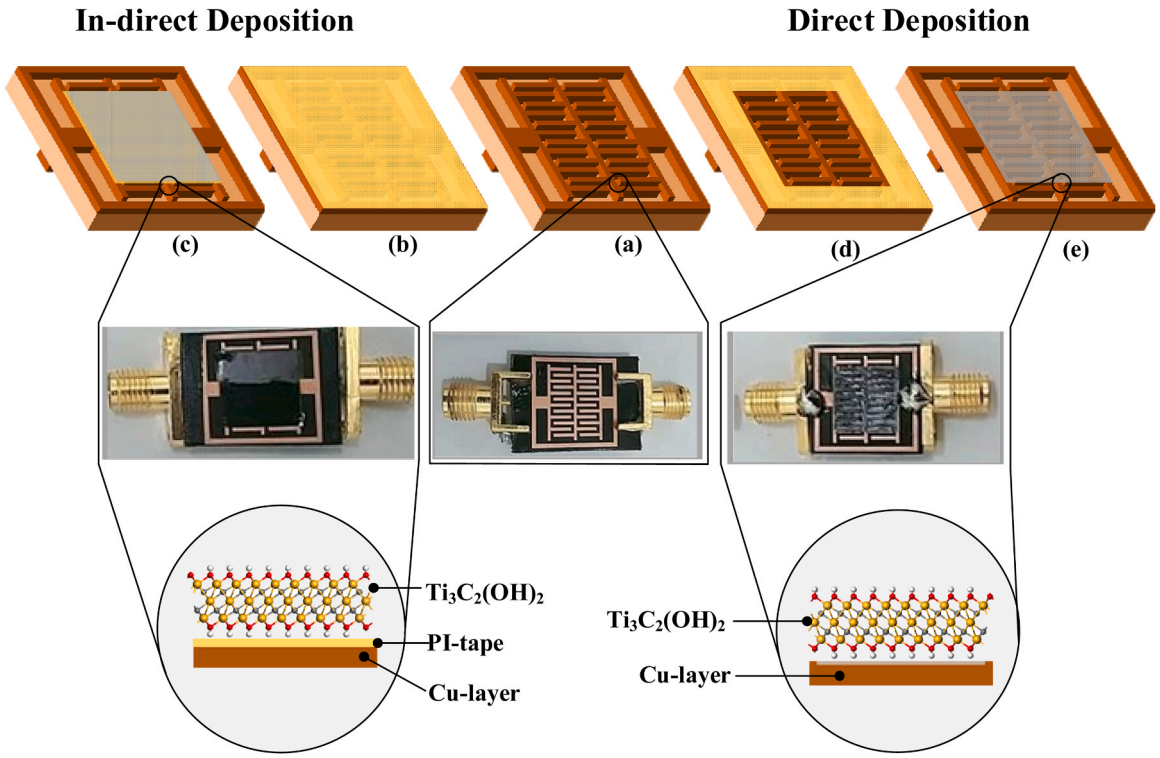

Fig. 2. (a) The proposed microwave resonator ground plane, (b) PI tape on the whole microwave resonator to avoid MXene film again from the zone around the interdigital fingers and place MXene on the sensing zone with a particular gap via PI tape (thickness 0.04 mm), (c) removing PI tape carefully around the sensing zone after placing MXene film on the interdigital fingers, (d) PI tape around the interdigital fingers to avoid extra sensing MXene film from it, and (e) placing sensing MXene film on the interdigital fingers and removing the PI tape around the interdigital fingers carefully so that the below copper layer is not damaged,.

chamber. To generate gas vapor at a precise concentration, a calculated amount of liquid acetone was injected into a plate inside the chamber using a microliter syringe, which was then turned into vapors and distributed uniformly by switching on a fan for 5 min. The gas chamber was equipped with a standardized temperature sensor (XC–24–K–12, Omega) and humidity sensor (HIH–4000, Honeywell). Additionally, a humid-temp RS 232 m was utilized to continuously monitor the temperature and humidity levels. The temperature was monitored throughout the experiment and compared to the sensor response, which remained constant and slightly impacted the sensor response. Before the next test, the vacuum pump was additionally used to release the loaded gas and reestablish the natural environment. A computer was connected to the gas chamber controller and VNA to compare, evaluate, and store sensor data. Furthermore, an I-V characteristic of the designed resonator was investigated by supplying varying levels of DC supply (MT-152D) to an interdigital capacitor with a coated layer of MXene and measuring

the resulting current flow (a digital multimeter, 3803). The measured data is then plotted on a graph to obtain the I-V curve, demonstrating the performance of a designed resonator for bare and under 100 ppm acetone gas exposure.

3. Results and Discussion

3.1. Morphological and structural characterization of MXene nanosheets

The $Ti_3C_2T_x$ MXene film Fourier transform infrared (FTIR) spectrum and X-ray diffraction ((XRD) Model D8X-Ray Diffractometer) patterns were detailed using Cu Kα radiation through a diffractometer (Fig. 3(a) and (b)). The scanning electron microscopic ((SEM) Model JEOL) graphs examined the sample's microstructure (Fig. 3(d) and 3 (e)). Fig. 3(d) illustrates the top view morphology of the $Ti_3C_2T_x$ MXene film with two different magnifications exhibiting a smooth surface with small mini ripples without any clear cracks. As the SEM picture illustrates the Mxene layer's cross-section in Fig. 3(f), the deposited MXene layer was 10 μm thick. Additionally, the DC electrical conductivity of $Ti_3C_2T_x$ MXene film, as measured by a low resistivity meter, was 2448.13 S/cm, significantly higher than graphene and other carbon nanotubes (see Supplementary Table S1).

For the gas-sensing performance of $Ti_3C_2T_x$ MXene, various functional groups are investigated due to their diverse adsorption energy against acetone gas molecules. The Density Function Theory (DFT) calculations are performed using theoretical models of $Ti_3C_2T_x$ MXene with three different functional groups (T_x = OH, O, F). Fig. 4(a) depicts the most stable configuration of the acetone molecule being adsorbed on the surface of OH-, O-, and F-terminated Ti_3C_2 MXene. It is found that the adsorption energies of $Ti_3C_2(OH)_2$, $Ti_3C_2O_2$, and $Ti_3C_2F_2$ for acetone molecules are − 1.33 eV, − 0.70 eV, and − 0.51 eV, respectively. This analysis indicates that the $Ti_3C_2(OH)_2$ possesses the highest binding energy for the acetone than other terminated MXenes. As per the experimental design, the binding energies between the $Ti_3C_2T_x$ against the methanol, ethanol, and acetone gases were further investigated and compared. The schematic of the most favorable fully relaxed configuration of gases (methanol and ethanol) on the $Ti_3C_2T_x$ is presented in Fig. 4(b) and (c) and Supplementary Fig. S3 and S4. Negative adsorption energy indicates that the adsorption process is the most energetically favorable from the experimental point of view, and the $Ti_3C_2(OH)_2$ has the strongest binding energy for gases compared to its counterparts, i.e., $Ti_3C_2O_2$ and $Ti_3C_2F_2$ as shown in Fig. 5. Therefore, a microwave sensor using OH-terminated MXene was developed for experimental investigation. The theoretical model of $Ti_3C_2T_x$ (OH termination) depicts that the adsorption energy for acetone is very high at 1.33 eV, which makes it difficult for the molecules to desorb at room temperature. The findings are compared with other studies that report lower values for similar analytes [39–41].

3.2. Effect of gas concentration on sensor response

The proposed MXene-based microwave sensor is more sensitive toward acetone than other VOCs due to the lower bond length and the high negative binding energy between the gas molecule and sensing film. The acetone gas with different concentrations was exposed to $Ti_3C_2T_x$ film-based microwave resonator at room temperature (RT) in a gas chamber (Fig. S2). The variation in the concentration of acetone gas is spotted through a significant alteration in the resonance frequency and amplitude of the designed sensor (Fig. 6). The sensitivity of sandwiching a PI tape between the sensing interface material and microwave resonator is enhanced more towards acetone gas than employing sensing film over the resonator. The high sensitivity of the indirect deposition of MXene-based resonator towards acetone gas is due to increased field distribution of the ELC structure and the gas detection sensitivity, which is the ratio of the alteration in resonant frequency caused by gas interaction to the resonant frequency ($\Delta f_R/f_R$). As a result, the ratio of capacitance change to net capacitance ($\Delta C_R/C_R$) increases dramatically, resulting in a more significant variation in the resonator's resonance frequency and amplitude.

Multi-parametric alterations in frequency shift, amplitude shift, and bandwidth broaden and loaded Q-factor is applied to estimate the sensitivity analysis of the developed MXene-based microwave sensor for monitoring low acetone gas concentration. Therefore, the precision of the detection method is improved by evaluating the statistical

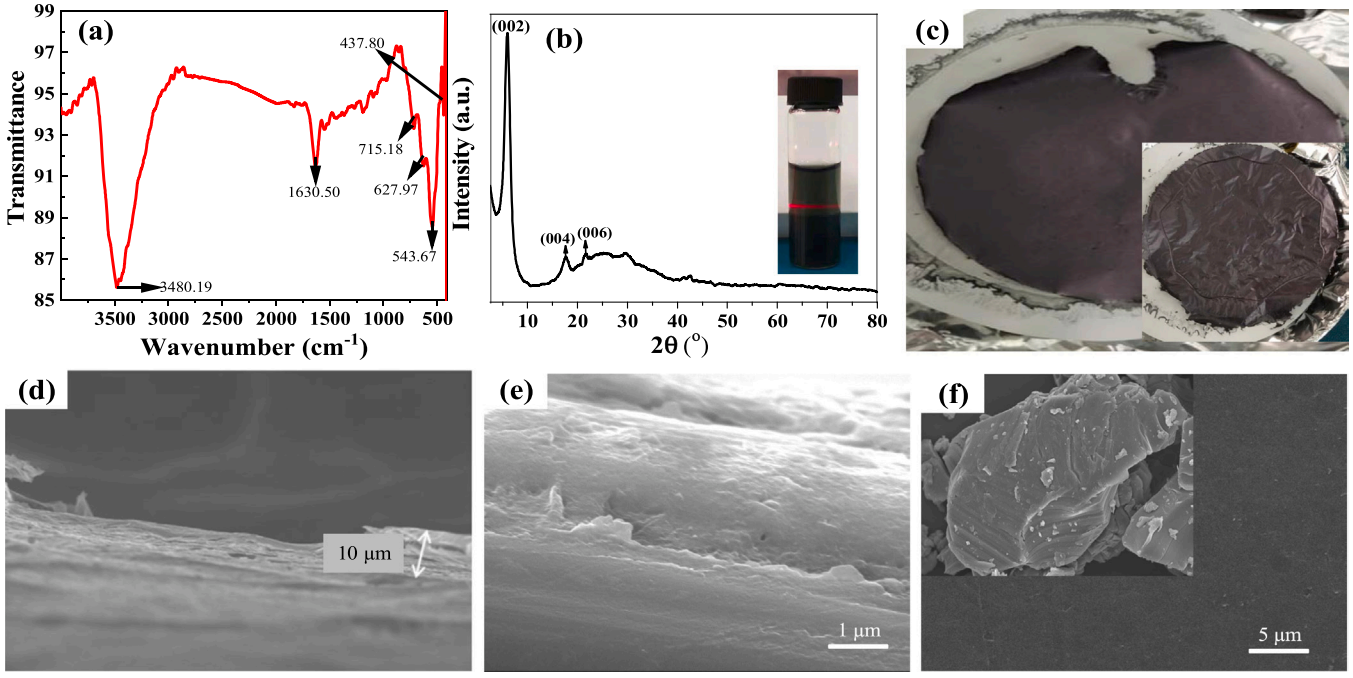

Fig. 3. (a) FTIR spectrum of $Ti_3C_2T_x$ MXene, (b) XRD pattern of $Ti_3C_2T_x$ Mxene, (c) MXene-film prepared, (d) SEM micrographs of MAX, (e) $Ti_3C_2T_x$ MXene top view morphology, and (f) cross-section of $Ti_3C_2T_x$ MXene.

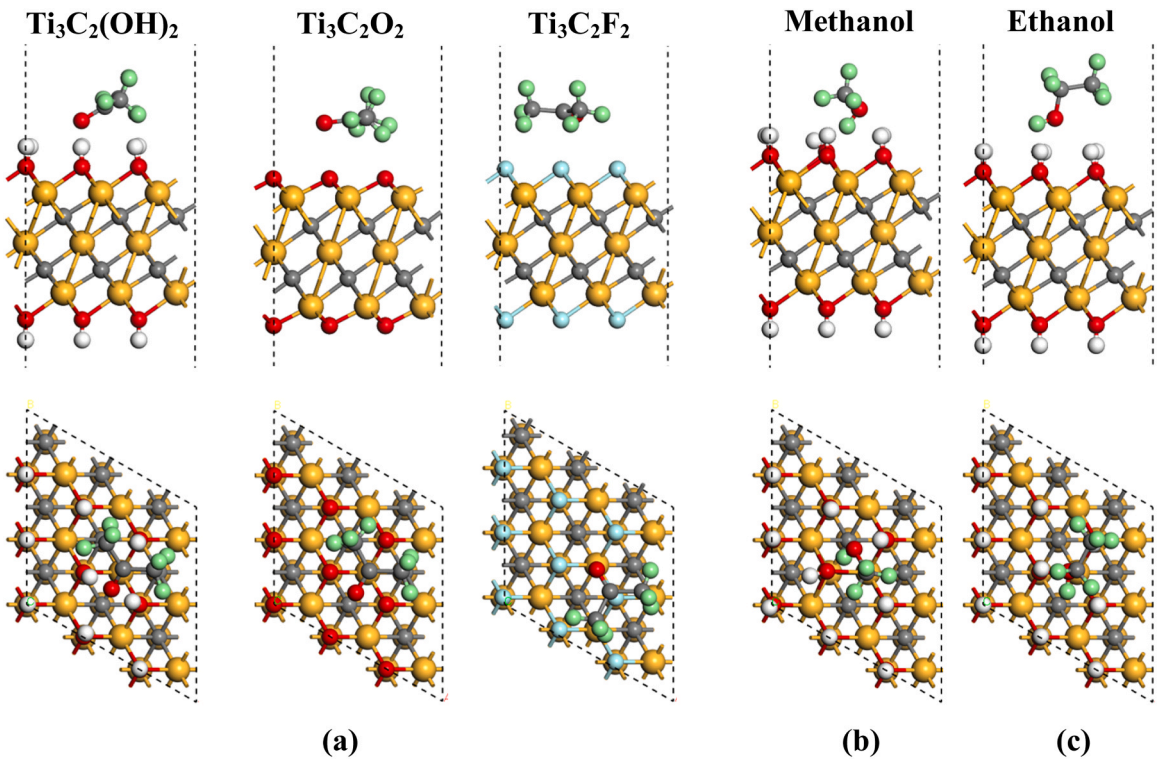

Fig. 4. Side and top schematics of the most stable configuration of (a) acetone absorbed on the $Ti_3C_2(OH)_2$, $Ti_3C_2O_2$, and $Ti_3C_2F_2$, (b) methanol, and (c) ethanol, on the $Ti_3C_2(OH)_2$ MXene.

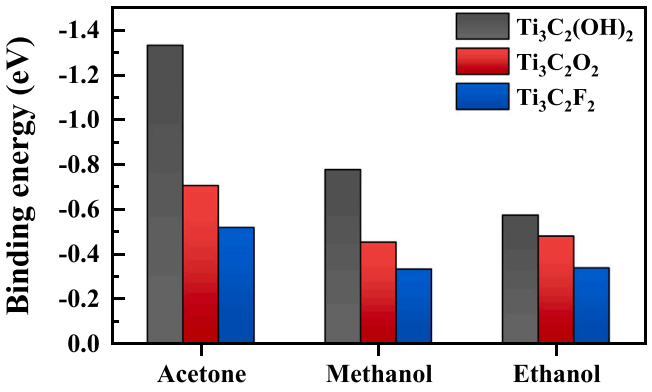

Fig. 5. Adsorption energies of acetone, methanol and ethanol on the surface of $Ti_3C_2T_x$ (T_x = OH, O, and F) MXene.

assessment of the sensitivity parameters individually. The applied linear regression strongly correlates with frequency shift and acetone gas concentration, with $r^2 = 0.97$ (r = correlation coefficient), as shown in Fig. 7(a). Similarly, the conductivity and impedance mismatching losses of the ELC resonator structure can be determined by examining the wave amplitude reduction as a function of acetone gas concentration. Fig. 7(b) shows a linear regression plot of amplitude change versus acetone gas concentration, indicating a strong correlation $r^2 = 0.93$ between wave amplitude reduction and acetone gas concentration.

Further, the bandwidth and Q factor (energy storage characteristics) have been studied to investigate the effect of acetone gas concentration on the proposed device's electric-field storage capability. With a limited 3 dB bandwidth and a constant phase near resonance, the low 3 dB bandwidth demonstrates outstanding frequency selection [42]. The ELC resonator structure's narrow bandwidth makes it more sensitive to tiny changes in energy loss in the sensing material. When a single gas molecule contacts MXene film, these energy losses cause phase resonance and electric field capacity to be disrupted, resulting in a shift in device sensitivity. As illustrated in Fig. 7(c), the computed linear regression demonstrates a good correlation of $r^2 = 0.95$ between wave bandwidth and acetone gas concentration. The sensing material's permittivity, shape, and volume on top of the ELC resonator structure influence the Q-factor shift [43]. The volume of the sensing material is fixed in the proposed device; the only parameter that can alter the Q-factor and exhibit device sensitivity is the permittivity of the sensing material. The high Q-factor causes a perturbation in the sensing zone due to existing acetone gas molecules interacting, resulting in a deflection in the Q-factor and showing in device sensitivity [44]. However, while a high Q-factor improves the microwave sensor's sensitivity, accuracy, and resolution, it also diminishes as the dielectric constant of the sensing material changes, limiting the microwave device's test range [45]. As the concentration of acetone gas increases, the Q-factor value in the suggested microwave sensor alters, as illustrated in Fig. 7(d). The presented linear regression reveals the strong correlation $r^2 = 0.98$ between the Q-factor value and acetone gas concentration.

3.3. Gas sensing performance of MXene-based microwave sensor

The interaction capability of acetone gas molecules with the MXene sensing film determines the developed sensor's response and recovery time. The sensor's response and recovery time are determined by the attachment and release of acetone gas ions, respectively. Furthermore, the MXene film was deposited directly and indirectly (through PI tape) on the enhanced electric field zone, resulting in dielectric losses, localized thermal agitation, and a short molecular separation time [46]. At microwave frequency, the interaction between heat dissipation factors and enhanced electric field can be represented as [47]:

$$\dot{H}_d = 2 \times \pi \times f_r \times \varepsilon_0 \times \tan(\delta) \times E_{rms}^2 \quad (1)$$

where H_d is the heat dissipation factor, ε_0 is free space permittivity $(8.54 \times 10^{-12}\ F/m^2)$ and E_{rms} is indicated by the root-mean-squared

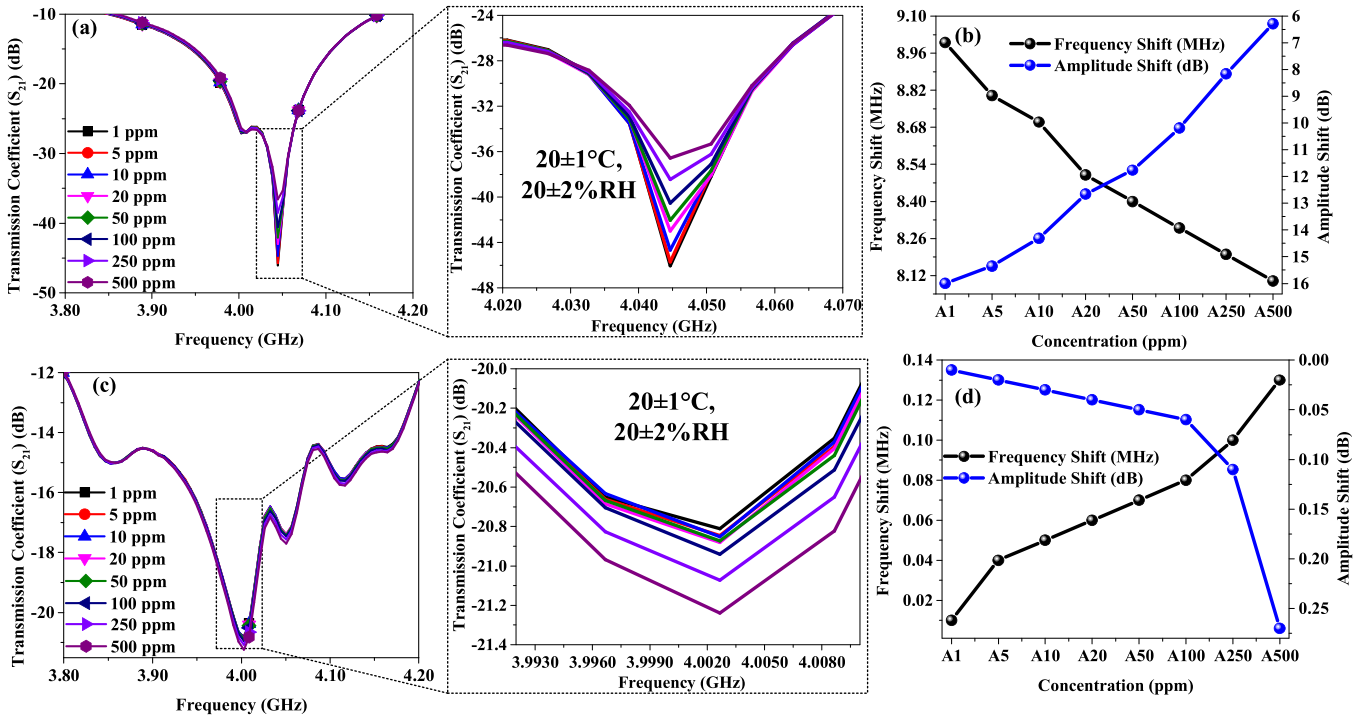

Fig. 6. (a) $|S_{21}|$ behavior of MXene deposition with PI tape on the designed sensor for acetone gas low concentration, (b) frequency and amplitude shift indirect MXene deposition on the proposed sensor (acetone gas concentration), (c) $|S_{21}|$ behavior of MXene deposition without PI tape on the resonator, and (d) frequency and amplitude shift for MXene deposition without PI tape on the resonator (acetone gas concentration).

value of the electric field in the sensing zone. Fig. 8(a) depicts the measurement response and recovery time of the designed MXene sensor. The response and recovery times for the developed MXene-based interdigital microwave sensor are estimated to be 60 and 85 s, respectively.

The repeatability test is essential for analyzing the sensor's behavior in multiple assessments of identical samples in the same environment. The high repeatability suggests that the sensor offers significant accuracy and resolution. As shown in Fig. 8(b), the developed MXene-based interdigital microwave sensor has experimented with quadruplicate samples of 250 ppm acetone gas concentration injected in the measuring chamber at various time intervals under RT. The measurement findings show that the output results are the same for each sample, indicating a significant level of repeatability. At 250 ppm, the maximum relative standard deviation (RSD) of 0.01% demonstrates good reproducibility in all analyzed specimens. The stability parameter must be investigated before implementing the gas sensor in practical uses [48]. The reported MXene-based microwave gas sensor was tested for seven days at 250 ppm acetone gas concentration in the same environment. Fig. 8(c) depicts the measurement result, which shows that the tested gadget had correlated sensing output for all seven days. The optimum RSD is 0.01% at an acetone gas concentration of 250 ppm, indicating exceptional lengthy stability.

In a gas sensing application, selectivity is an essential parameter, which is described as the ability of a gas sensor to respond to the targeted gas molecule in the presence of different gases. The term selectivity coefficient (K) of the designed sensor can be calculated as [49]:

$$K = \frac{S_{Acetone}}{S_{VOC}} \quad (2)$$

$S_{Acetone}$ is the response of the designed sensor towards acetone gas in the existence of other VOCs gases (S_{VOC}). The variation in the resonance frequency and amplitude of the $Ti_3C_2T_x$ film-based microwave sensor is observed under the contact of 250 ppm of acetone methanol, ethanol, xylene, and toluene, as shown in Fig. 8(d). The designed sensor is more sensitive to the acetone gas due to more negative adsorption energies and a small bond length between the molecule and sensing layer than other VOC gases. The binding energies between the $Ti_3C_2T_x$ against the methanol, ethanol, and acetone gases were further investigated and compared, which depicts that the MXene with OH termination is more sensitive towards acetone due to lower bond length and further the experimental results also indicated that the selectivity of the designed sensor towards 250 ppm acetone concentration is high as compared to other gases as shown in Fig. 8(d). The selectivity of VOCs for the designed sensors is in the order of acetone > methanol > ethanol which is consistent with the theoretically predicted binding energies of these VOCs. Furthermore, the humidity impact on the designed sensor frequency and amplitude shift is illustrated in Fig. 8(e) and (f). The sensor can still detect acetone gas even though greater humidity values would produce a slight reduction in the gas response. In Table 1, a comparison is made between the proposed interdigital MXene-based resonators with other reported gas sensors based on microwave technology. This study demonstrates that incorporating a PI film produced a strong EM field between the interdigital capacitor structure of the resonator and the MXene layer, leading to a substantial interaction between the resonator's EM field and acetone gas molecules through the MXene layer. The designed microwave gas sensor based on MXene exhibits twice as high sensitivity as the one without PI tape, enabling it to detect acetone gas concentration more accurately. The limit of detection of the immobilized MXene-based microwave sensor with PI tape is 0.923 ppm.

4. Mechanism of Gas Sensing and Microwave Response

The high-sensitivity planar microwave resonator gas sensor operates based on the enhanced interaction between the resonator's EM field and the surrounding target gas via the immobilized $Ti_3C_2T_x$ MXene. Immobilizing an MXene layer in the resonator structure offers an effective wide open area with high-density active sites for absorbing target gas molecules, thereby enhancing the interaction between the resonator's EM field and target gas. However, a challenge with a conductive MXene

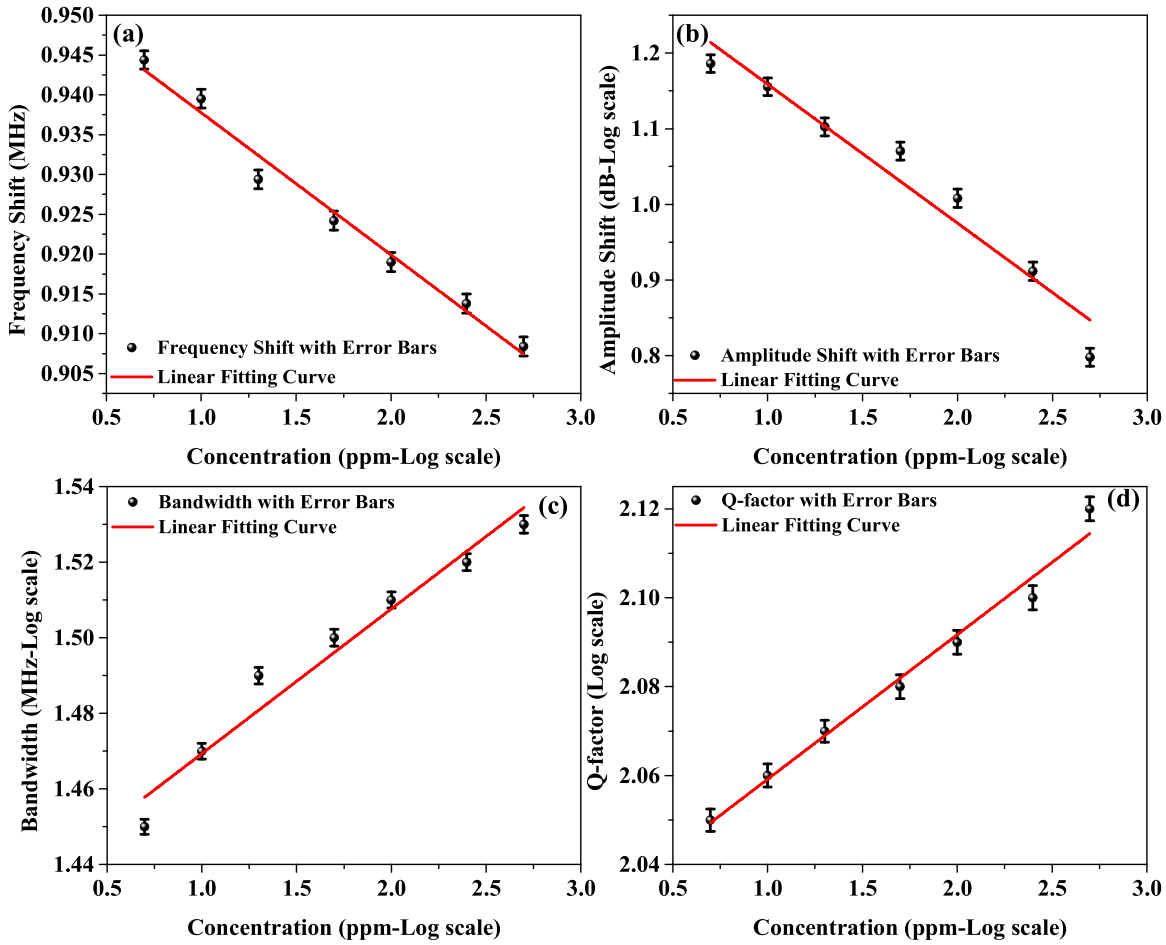

Fig. 7. Linear regression plot of a designed MXene-based microwave sensor with PI tape for (a) frequency shift, (b) amplitude shift, (c) bandwidth (BW), and (d) Q-factor as per logarithmic scale of the MXene-based microwave sensor for indirect deposition concerned with different acetone concentrations.

layer immobilized directly on the resonator surface lies in the impact of its EM loss on the resonant profile, adversely affecting the gas detection sensitivity. To overcome this challenge, the MXene layer was first deposited on a PI film, which was later attached to the resonator's surface. Sandwiching a PI film confined an intense EM field between the resonator's IDC metal lines and MXene, which significantly enhanced the interaction of the field with the target gas. The interaction between the resonator's EM field and the target gas via the MXene layer alters the resonator's spectral parameters, such as resonant frequency, resonant amplitude, and quality factor. These parameters, which correlate with the relative permittivity and EM loss of the MXene layer interacting with gases, can be used to detect and characterize the target gas. A circuit model was implemented in Advanced Design System by Keysight to analyze the sensitivity-enhanced gas detection performance of the sensor, as shown in Supplementary Fig. S5. The values of circuit model components in the resonator structure with immobilized MXene layer were calculated using the following equations:

$$L_R = \frac{60l}{v_0} ln\left[\frac{8h}{w} + \frac{w}{4h}\right] \quad for \quad \frac{w}{h} \leq 1 \tag{3}$$

where L_R represents the microstrip line inductance of the resonator's outer ring, l and w represent the length and the width of the microstrip line, respectively, and h is the height of the substrate.

$$C_{IDC} = (C_{Sub} + C_D)(N-1)L = \left[\frac{\varepsilon_0 \varepsilon_{Sub}\sqrt{K\left(1-k^2\right)}}{K(k)} + \frac{\varepsilon_0 t}{a}\right](N-1)L \tag{4}$$

where C_D and C_{Sub} are the capacitances due to the electric flux passing between the IDC fingers directly and via the underlying substrate. N is the number of coupled fingers in IDC, and L is the coupled length of the fingers. ε_0 is the absolute permittivity of air, and ε_{sub} (=3.5) is the relative permittivity of the RF-35 substrate. k and $K(k)$ are the elliptical integrals of the first kind. C_{MX} [$= \varepsilon_0\varepsilon_{PI}(ab/t_{PI})$] is the capacitance due to the flux passing between the IDC fingers and MXene layer through the PI film, where ε_{PI} (= 2.7) and t_{PI} (= 40 μm) are the dielectric constant and thickness of the PI film, respectively, and ε_{PI} (= 2.7) is the relative permittivity of the PI film.

The resonator's inductance and capacitance values were calculated using the abovementioned equations. According to Eqs. (3) and (4), the total capacitance (C_{IDC}) and inductance (L_R) of the interdigital structure were estimated as 10 pF and 0.51 nH, respectively. Using the values of inductance and capacitance, the resonant frequency (f_R) of the resonator sensor with the immobilized MXene layer can be calculated using the following equation:

$$f_R = \frac{1}{2\pi\sqrt{L_R C_R}} = \frac{1}{2\pi\sqrt{L_R\left[\frac{C_{IDC}C_{MX}}{C_{IDC}+C_{MX}}\right]}} \tag{5}$$

where C_R is the net capacitance of the resonator sensor. As Eq. (5) indicates, immobilizing the MXene layer on the resonator sensor via a sandwiched PI film decreases the net capacitance of the resonator. Consequently, the gas detection sensitivity (S), which is the ratio of the change in the sensor's resonant frequency due to exposure to gas and the bare resonant frequency ($\Delta f_R/f_R$), and therefore, the ratio of the change

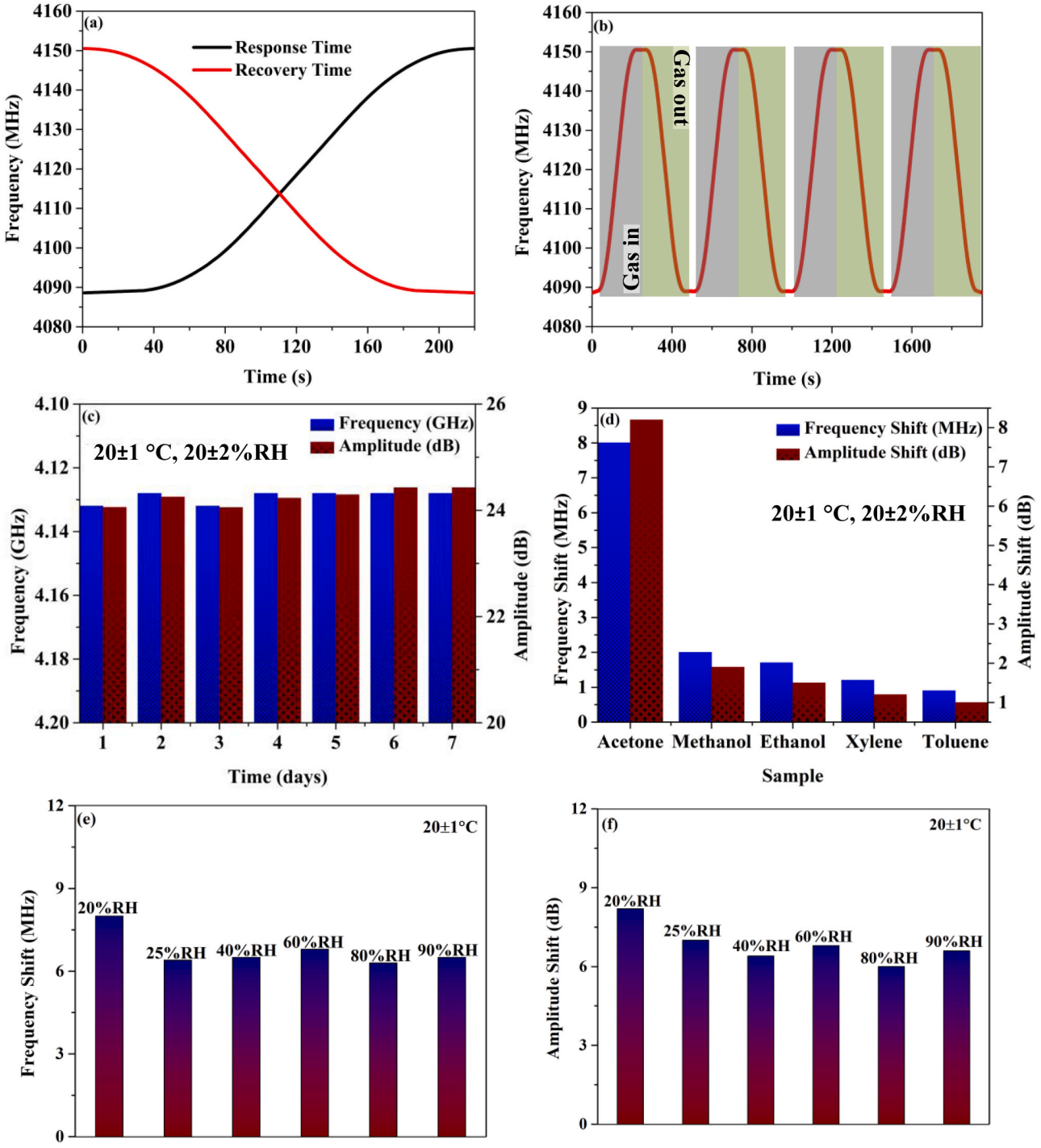

Fig. 8. MXene-based microwave gas sensor performance with PI tape (a) Response and recovery time, (b) repeatability, (c) stability, (d) selectivity of the MXene-based microwave sensor towards 250 ppm acetone gas concentrations, (e) frequency and (f) amplitude shift response of the sensor to 250 ppm acetone gas under different relative humidity at 20 ± 1 °C.

in capacitance and the net capacitance ($\Delta C_R/C_R$), increases significantly. Furthermore, the sensitivity of the proposed sensor with the MXene layer deposited directly on the resonator surface and with the MXene layer deposited on the PI substrate and attached to the resonator surface was determined. The MXene layer interacting with gas was modeled with relative permittivity ranging from 1 to 10 by carefully choosing the values of C_{MX}. As Fig. S6 presents, the sensitivity (the slope of the resonant frequency versus relative permittivity plot) of the MXene-PI layer-immobilized resonator sensor (0.01538 GHz/ε_r) was 1.4 times the sensitivity with the MXene-deposited resonator sensor (0.00281 GHz/ε_r), thereby validating the proposed concept.

Gas adsorption is the primary cause of changes in conductivity observed in the sensing layers. This phenomenon induces local deformations in the MXene material, which alters bond lengths and modulates electrical conductivity [54]. It is well-known that gas molecules can interact with the surface of materials, causing changes in the electronic structure and properties of the material. In the case of MXene, gas adsorption-induced deformations lead to changes in the effective charge carrier concentration, band structure, and bandgap of the material. These changes subsequently affect the material's electrical

Table 1
Comparison of the performance of the proposed MXene-based interdigital sensor with various reported microwave gas sensors.

Gas-Sensitive Material	Sensor Structure	Sensitivity	Detection Range	Ref
PIn/APS	Substrate integrated waveguide	3.35 kHz/ppm	5–500 ppm	[3]
Poly copolymer films	Coplanar waveguide	0.104 kHz/ppm	700–2000 ppm	[13]
Phthalocyanine (Pc)	Interdigital	14 MHz/ppm	5–25 ppm	[16]
Polydimethylsiloxane	Split ring resonator	0.194 kHz/ppm	387–1935 ppm	[26]
MXene	Planar antenna	0.7 MHz/ppt	0.00008%–0.0008%	[38]
PEDOT: PSS	Differential capacitive	2.153 kHz/ppm	500–1300 ppm	[50]
Carbon nanotubes	Interdigital	648.1 Hz/ppm	625–5000 ppm	[51]
P25DMA polymer	Resonant cavity	2.33 mdB/ppm	625–5000 ppm	[52]
Reduced graphene oxide	Split ring resonator	0.9 MHz/ppm	100–400 ppm	[53]
MXene	Planar interdigital	17.85 kHz/ppm (MXene via PI film) and 8.23 kHz/ppm (MXene without PI film)	1–500 ppm	This work

conductivity. Our findings provide insight into the fundamental mechanisms governing the electrical response of MXene-based gas sensors, which is significant for developing high-performance gas sensing devices. The behavior of acetone gas molecules adsorbing onto the MXene film alters the resistivity of the sensing interface material. The change in resistivity of a sensing film is detected through a change in the resonant frequency and amplitude of the sensor response of a microwave resonator, which is used to monitor the existence of acetone gas. The change in frequency that occurs during each adsorption sequence is directly related to the sensing mechanism of the $Ti_3C_2T_x$ MXene [36]. This mechanism involves the adsorption of gas molecules by the functional groups and structural defects present in the MXene. Consequently, the frequency shift observed is directly related to this mechanism, as it is affected by the interaction between the MXene and the gas molecules. Therefore, by monitoring the frequency shift during adsorption, it is possible to gain insight into the sensing mechanism of the $Ti_3C_2T_x$ MXene, which has potential applications in gas sensing technology.

The electrical characteristics of immobilized MXene nanocomposites on the interdigital structure of the designed sensor are characterized and observed via current-voltage (I-V) response, as shown in Fig. S7. The I-V response of the MXene-based microwave sensor exhibited an ohmic resistance type electrical behavior. A linear electrical response is examined for the designed sensor, and the current remains constant regardless of the applied voltage for a bare sensor. Similarly, the designed sensor response was examined upon exposure to 100 ppm acetone gas, and the variation in the resistance decreased in contrast to the bare sensor concerned with applied voltage. Thus, the resistance changes when the MXene is exposed to acetone gas concentration and is exhibited through the designed sensor's transmission coefficient (dB).

5. Conclusion

To sum up, this work investigated the potential of MXene as a gas-sensitive interface in a planar microwave resonator sensor for detecting acetone gas with high sensitivity, selectivity, linearity and good humidity resistance at room temperature (20 ± 1 °C, 20 ± 2%RH). In contrast to the conventional approach to implement microwave gas sensors, where gas-sensitive material is immobilized directly on the resonator surface, noncontact immobilization of MXene on the resonator surface via a PI substrate was proposed to enhance the sensitivity to detect acetone gas significantly. Embedding a PI film between MXene and the resonator sensor enhanced the acetone gas detection sensitivity by confining the EM field. The resonant frequency and amplitude are the main sensing parameters for detecting acetone gas concentrations ranging from 500 to 1 ppm. The DFT calculation is employed for investigating the performance of the sensing interface material, which exhibits that the $Ti_3C_2T_x$ (T_x = OH) layer is more sensitive toward monitoring low-concentration acetone gas. The high sensitivity of the designed sensor towards monitoring low concentrations of acetone gas is due to more negative binding energy, indicating a small bond length between the acetone gas molecule and sensing interface film compared with $Ti_3C_2T_x$ (T_x = O and F). The measurement results show that the proposed MXene-based microwave interdigital sensor has great potential for monitoring acetone gas. In the future, the emphasis would be on improving the sensing parameter by upgrading the sensing interface material and design layout and replacing PI tape with another nanomaterial to enhance further the sensitivity and selectivity of the designed sensor suitable for biomedical and industry-related technologies.

Supporting Information

The supporting information contains detailed information on the experimental method, which includes materials and instruments, microwave sensor design, and measurement setup. Additionally, the figures conclude the proposed interdigital structure with dimension marker and electric field distribution, resonating frequency comparison with/without PI tape deposition of MXene, electric field distribution and 2-D schematic of the VOC gas chamber. The supporting information file is available free of charge.

CRediT authorship contribution statement

Luqman Ali: Conceptualization, Methodology, Software, Validation, Formal analysis, Investigation, Data curation, Visualization, Writing. **Jie Wei**: Methodology, Software, Validation, Formal analysis, Investigation, Data curation, Visualization, Writing. **Fan-Yi Meng:** Visualization, Project administration, Funding acquisition. **Muhammad Waqas Qureshi**: Software. **Kishor Kumar Adhikari:** Conceptualization, Methodology, Software, Validation, Formal analysis, Investigation, Data curation, Visualization, Writing. **Ming-Yu Li**: Formal analysis, Investigation. **Jun-Ge Liang:** Validation, Resources, Data curation. **Xiao-Long Wang**: Investigation, Data curation. **Xu-Min Ding:** Formal analysis. **Nam-Young Kim:** Validation. **Cong Wang**: Conceptualization, Methodology, Validation, Formal analysis, Investigation, Resources, Data curation, Visualization, Supervision, Project administration, Funding acquisition, Writing.

Declaration of Competing Interest

The authors declare that they have no known competing financial interests or personal relationships that could have appeared to influence the work reported in this paper.

Data Availability

Data will be made available on request.

Acknowledgement

This research was supported by the National Key Research and Development Program of China (2021YFF0603500 and 2019YFE0121800), the National Natural Science Foundation of China

(Grant No. 61971160, 62271229 and U22A2014), the Project of Jilin Province Development and Reform Commission (Grant No. 2022C047–6) and the Project of Science and Technology Development Program of Changchun City (Grant No. 21ZY23). This research was also partially supported by Basic Science Research Program through the National Research Foundation of Korea (NRF), funded by the Ministry of Education (No. 2018R1A6A1A03025242) and a Research Grant from Kwangwoon University 2023. We want to give our heartfelt thanks to everyone who has ever helped us with this paper, especially Fan Yang, Yang Yi, Xiong Yu, De-Shuai Meng, Jia-Kang Wu, Shi-Peng Jiang, Zhe-Yi Li and Eun-Seong Kim.

Appendix A. Supporting information

Supplementary data associated with this article can be found in the online version at doi:10.1016/j.snb.2023.134048.

References

[1] S. Shen, Z. Fan, J. Deng, X. Guo, L. Zhang, G. Liu, Q. Tan, J. Xiong, An LC passive wireless gas sensor based on PANI/CNT composite, Sensors 18 (2011) 3022.
[2] N.R. Tanguy, B. Wiltshire, M. Arjmand, M.H. Zarifi, N. Yan, Highly sensitive and contactless ammonia detection based on nanocomposites of phosphate-functionalized reduced graphene oxide/polyaniline immobilized on microstrip resonators, ACS Appl. Mater. Interfaces 12 (2020) 9746–9754.
[3] A. Kumar, C. Wang, F.Y. Meng, C.P. Jiang, G.F. Yan, M. Zhao, C.Q. Jing, L. Wang, Ultrafast detection and discrimination of methanol gas using a polyindole-embedded substrate integrated waveguide microwave sensor, ACS Sens. 5 (2020) 3939–3948.
[4] M.H. Zarifi, M. Fayaz, J. Goldthorp, M. Abdolrazzaghi, Z. Hashisho, M. Daneshmand, Microbead-assisted high resolution microwave planar ring resonator for organic-vapor sensing, Appl. Phys. Lett. 106 (2015), 062903-1-4.
[5] K.K. Adhikari, C. Wang, T. Qiang, Q. Wu, Polyimide-derived laser-induced porous graphene-incorporated microwave resonator for high-performance humidity sensing, Appl. Phys. Express 12 (2019), 106501-1-5.
[6] H. Yu, C. Wang, F.Y. Meng, J.G. Liang, H.S. Kashan, K.K. Adhikari, L. Wang, E. S. Kim, N.Y. Kim, Design and analysis of ultrafast and high-sensitivity microwave transduction humidity sensor based on belt-shaped MoO_3 nanomaterial, Sens. Actuators B Chem. 304 (2020), 127138-1-10.
[7] C. Chen, K.D. Campbell, I. Negi, R.A. Iglesias, P. Owens, N. Tao, F. Tsow, E. S. Forzani, A new sensor for the assessment of personal exposure to volatile organic compounds, Atmos. Environ. 54 (2012) 679–687.
[8] X. Zhou, Z. Xue, X. Chen, C. Huang, W. Bai, Z. Lu, T. Wang, Nanomaterial-based gas sensors used for breath diagnosis, J. Mater. Chem. B 8 (2020) 3231–3248.
[9] J. Zuo, J. Feng, M.G. Gameiro, Y. Tian, J. Liang, Y. Wang, J. Ding, Q. He, RFID-based sensing in smart packaging for food applications: a review, Futur. Foods 6 (2022), 100198-1-16.
[10] S. Dhall, B.R. Mehta, A.K. Tyagi, K. Sood, A review on environmental gas sensors: materials and technologies, Sens. Int 2 (2021), 100116-1-10.
[11] S.K. Singh, P. Azad, M.J. Akhtar, K.K. Kar, Improved methanol detection using carbon nanotube-coated carbon fibers integrated with a split-ring resonator-based microwave sensor, ACS Appl. Nano Mater. 1 (2018) 4746–4755.
[12] A. Rydosz, A. Brudnik, K. Staszek, Metal oxide thin films prepared by magnetron sputtering technology for volatile organic compound detection in the microwave frequency range, Mater. (Basel) 12 (2019), 877-1-13.
[13] H. Li, Z. Chen, N. Borodinov, Y. Shao, I. Luzinov, G. Yu, P. Wang, Multi-frequency measurement of volatile organic compounds with a radio-frequency interferometer, IEEE Sens. J. 17 (2017) 3323–3331.
[14] M. Righettoni, A. Tricoli, Toward portable breath acetone analysis for diabetes detection, J. Breath. Res 5 (2011), 037109-1-8.
[15] H. Niu, P. Yu, Y. Zhu, Z. Jing, P. Li, B. Wang, C. Ma, J. Wang, J. Wu, A.O. Govorov, A. Neogi, Z.M. Wang, Mach-Zehnder interferometer based integrated-photonic acetone sensor approaching the sub-ppm level detection limit, Opt. Express 30 (2022), 29665-1-14.
[16] A. Rydosz, E. Maciak, K. Wincza, S. Gruszczynski, Microwave-based sensors with phthalocyanine films for acetone, ethanol and methanol detection, Sens. Actuators B Chem. 237 (2016) 876–886.
[17] A.J. Saraf, E. Hosseini, B.D. Wiltshire, M.H. Zarifi, M. Arjmand, Graphene oxide/polyaniline-based microwave split-ring resonator: a versatile platform towards ammonia sensing, J. Hazard Mater. 418 (2021), 126283-1-13.
[18] C. Wang, L. Ali, F.Y. Meng, K.K. Adhikari, Z.L. Zhou, Y.C. Wei, D.Q. Zou, H. Yu, High-accuracy complex permittivity characterization of solid materials using parallel interdigital capacitor-based planar microwave sensor, IEEE Sens. J. 21 (2021) 6083–6093.
[19] L. Ali, C. Wang, F.Y. Meng, K.K. Adhikari, Z.Q. Gao, Interdigitated planar microwave sensor for characterizing single/multilayers magnetodielectric material, IEEE Microw. Wirel. Compon. Lett. 32 (2022) 619–622.
[20] N.Y. Kim, K.K. Adhikari, R. Dhakal, Z. Chuluunbaatar, C. Wang, E.S. Kim, Rapid, sensitive and reusable detection of glucose by a robust radiofrequency integrated passive device biosensor chip, Sci. Rep. 5 (2015), 7807-1-9.
[21] K.K. Adhikari, C. Wang, T. Qiang, A. Kumar, Q. Wu, S. Maharjan, N.Y. Kim, Real-time accurate quantification of nanoliter ethanol using performance-optimized micro-fabricated microwave resonant sensor, J. Phys. D. Appl. Phys. 53 (2020), 085402-1-8.
[22] H. Lee, G. Shaker, K. Naishadham, X. Song, M. McKinley, B. Wagner, M. Tentzeris, Carbon-nanotube loaded antenna-based ammonia gas sensor, IEEE Trans. Microw. Theory Tech. 59 (2011) 2665–2673.
[23] T. He, W. Liu, T. Lv, M. Ma, Z. Liu, A. Vasiliev, X. Li, MXene/SnO_2 heterojunction based chemical gas sensors, Sens. Actuators B Chem. 329 (2021), 129275.
[24] H. Yu, C. Wang, F.Y. Meng, J. Xiao, J. Liang, H. Kim, S. Bae, D.Q. Zou, E.S. Kim, N. Y. Kim, M. Zhao, B.Q. Li, Microwave humidity sensor based on carbon dots-decorated MOF-derived porous Co_3O_4 for breath monitoring and finger moisture detection, Carbon 183 (2021) 578–589.
[25] M.H. Zarifi, A. Sohrabi, P.M. Shaibani, M. Daneshmand, T. Thundat, Detection of volatile organic compounds using microwave sensors, IEEE Sens. J. 15 (2015) 248–254.
[26] S. Mohammadi, M.H. Zarifi, Differential microwave resonator sensor for real-time monitoring of volatile organic compounds, IEEE Sens J. 21 (2021) 6105–6114.
[27] M.R. Lukatskaya, S. Kota, Z. Lin, M.Q. Zhao, N. Shpigel, M.D. Levi, J. Halim, P. L. Taberna, W.B. Barsoum, P. Simon, Y. Gogotsi, Ultra-high-rate pseudocapacitive energy storage in two-dimensional transition metal carbides, Nat. Energy 2 (2017) 17105.
[28] T. Yun, H. Kim, A. Iqbal, Y.S. Cho, G.S. Lee, M.K. Kim, S.J. Kim, D. Kim, Y. Gogotsi, S.O. Kim, C.M. Koo, Electromagnetic shielding of monolayer MXene assemblies, Adv. Mater. 32 (2020) 1–9.
[29] Z. Li, Y. Wu, 2D early transition metal carbides (MXenes) for catalysis, Small 15 (2019) 1–10.
[30] Y. Lei, W. Zhao, Y. Zhang, Q. Jiang, J.H. He, A.J. Baeumner, O.S. Wolfbeis, Z. L. Wang, K.N. Salama, H.N. Alshareef, A MXene-based wearable biosensor system for high-performance in vitro perspiration analysis, Small 15 (2019) 1–10.
[31] M.Q. Zhao, C.E. Ren, Z. Ling, M.R. Lukatskaya, C. Zhang, K.L.V. Aken, M. W. Barsoum, Y. Gogotsi, Flexible MXene/carbon nanotube composite paper with high volumetric capacitance, Adv. Mater. 27 (2015) 339–345.
[32] H. Chen, Y. Wen, Y. Qi, Q. Zhao, L. Qu, C. Li, Pristine titanium carbide MXene films with environmentally stable conductivity and superior mechanical strength, Adv. Funct. Mater. 30 (2020) 1–9.
[33] F. Shahzad, M. Alhabeb, C.B. Hatter, B. Anasori, S.M. Hong, C.M. Koo, Y. Gogotsi, Electromagnetic interference shielding with 2D transition metal carbides (MXenes), Science 253 (2016) 1137–1140.
[34] K. Khan, A.K. Tareen, M. Iqbal, Z. Ye, Z. Xie, A. Mahmood, N. Mahmood, H. Zhang, Recent progress in emerging novel MXenes based materials and their fascinating sensing applications, Small 2206147 (2023) 1–49.
[35] E.P. Simonenko, N.P. Simonenko, A.S. Mokrushin, T.L. Simonenko, P.Y. Gorobtsov, I.A. Nagornov, G. Korotcenkov, V.V. Sysoev, N.T. Kuznetsov, Application of titanium carbide MXenes in chemiresistive gas sensors, Nanomaterials 13 (2022) 850.
[36] E. Lee, A. Vahidmohammadi, B.C. Prorok, Y.S. Yoon, M. Beidaghi, D.J. Kim, Room temperature gas sensing of two-dimensional titanium carbide (MXene), ACS Appl. Mater. Interfaces 9 (2017) 37184–37190.
[37] S.J. Kim, H.J. Koh, C.E. Ren, O. Kwon, K. Maleski, S.Y. Cho, B. Anasori, C.K. Kim, Y. K. Choi, J. Kim, Y. Gogotsi, H.T. Jung, Metallic Ti_3C_2Tx MXene gas sensors with ultrahigh signal-to-noise ratio, ACS Nano 12 (2018) 986–993.
[38] K.K. Kazemi, S. Hu, O. Niksan, K.K. Adhikari, N.R. Tanguy, S. Li, M. Arjmand, M. H. Zarifi, Low-profile planar antenna sensor based on Ti_3C_2Tx MXene membrane for VOC and humidity monitoring, Adv. Mater. Interfaces 9 (2022), 2102411-1-11.
[39] M. Liu, J. Ji, P. Song, M. Liu, Q. Wang, α-Fe_2O_3 nanocubes/$Ti_3C_2T_x$ MXene composites for improvement of acetone sensing performance at room temperature, Sens. Actuators B Chem. 349 (2021), 130782.
[40] X. Tian, L. Yao, X. Cui, R. Zhao, T. Chen, X. Xiao, Y. Wang, A two-dimensional $Ti_3C_2T_X$ MXene @TiO_2/MoS_2 heterostructure with excellent selectivity for the room temperature detection of ammonia, J. Mater. Chem. A 10 (2022) 5505–5519.
[41] N.P. Simonenko, O.E. Glukhova, I.A. Plugin, D.A. Kolosov, I.A. Nagornov, T. L. Simonenko, A.S. Varezhnikov, E.P. Simonenko, V.V. Sysoev, N.T. Kuznetsov, The Ti0.2V1.8C MXene ink-prepared chemiresistor: From theory to tests with humidity versus VOCs, Chemosensors 11 (2023) 7.
[42] L. Crocco, P. Kosmas, Electromagnetic technologies for medical diagnostics: fundamental issues, clinical applications, and perspectives, MDPI (2019), 978-3-03897-676-9.
[43] A.W. Kraszewski, S.O. Nelson, T.S. You, Use of a microwave cavity for sensing dielectric properties of arbitrarily shaped biological objects, IEEE Trans. Microw. Theory Tech. 38 (1990) 858–863.
[44] S. Kiani, P. Rezaei, M. Navaei, M.S. Abrishamian, Microwave sensor for detection of solid material permittivity in single/multilayer samples with high-quality factor, IEEE Sens J. 18 (2018) 9971–9977.
[45] F. Li, Y. Zheng, C. Hua, J. Jian, Gas sensing by microwave transduction: review of progress and challenges, Front. Mater. 6 (2019) 1–12, 101.
[46] R. Cherbański, E. Molga, Intensification of desorption processes by use of microwaves-an overview of possible applications and industrial perspectives, Chem. Eng. Process. 48 (2009) 48–58.
[47] M. Regier, K. Knoerzer, H. Schubert. The Microwave Processing of Foods, second ed., Woodhead Publishing, 2016, pp. 978–0-081-00531-6.
[48] H. Nazemi, A. Joseph, J. Park, A. Emadi, Advanced micro and nano-gas sensor technology: a review, Sensors 19 (2019) 1285.
[49] M.A. Ryan, A.V. Shevade, C.J. Taylor, M.L. Homer, M. Blanco, J.R. Stetter. Computational Methods for Sensor Material Selection, first ed., Springer,, 2010, pp. 978–0-387-73715-7.

[50] P. Bahoumina, H. Hallil, J.L. Lachaud, A. Abdelghani, K. Frigui, S. Bila, D. Baillargeat, Q. Zhang, P. Coquet, C. Paragua, E. Pichonat, H. Happy, D. Rebière, C. Dejous, VOCs monitoring using differential microwave capacitive resonant transducer and conductive PEDOT: PSSMWCNTs nanocomposite film for environmental applications, IEEE Trans. Nanotechnol. 18 (2018).
[51] P. Bahoumina, H. Hallil, J.L. Lachaud, A. Abdelghani, K. Frigui, S. Bila, D. Baillargeat, A. Ravichandran, P. Coquet, C. Paragua, E. Pichonat, H. Happy, D. Rebière, C. Dejous, Microwave flexible gas sensor based on polymer multi wall carbon nanotubes sensitive layer, Sens. Actuators B. Chem. 249 (2017) 708–714.
[52] W.T. Chen, K.M.E. Stewart, R.R. Mansour, and A. Penlidis, Polymeric sensing material-based selectivity-enhanced RF resonant cavity sensor for volatile organic compound (VOC) detection, IEEE MTT-S Int. Microw. Symp. Dig. 2015 1–3.
[53] S.K. Singh, P. Azad, M.J. Akhtar, K.K. Kar, High-sensitive nitrogen dioxide and ethanol gas sensor using a reduced graphene oxideloaded double split ring resonator, Mater. Res. Exp. 4 (2017), 086301.
[54] W.Y. Chen, S.N. Lai, C.C. Yen, X. Jiang, D. Peroulis, L.A. Stanciu, Surface functionalization of $Ti_3C_2T_x$ MXene with highly reliable superhydrophobic protection for volatile organic compounds sensing, ACS Nano 14 (2020) 11490.

Luqman Ali received the bachelor's degree in electronics engineering from the University of Peshawar in 2015 and the master's degree in electrical engineering from Bahria University, Islamabad, Pakistan, in 2017. He is currently pursuing a Ph.D. with the School of Electronics and Information Engineering, Harbin Institute of Technology, Harbin, China. His research interests include RF microwave gas sensors, meta-material, antenna designation, and meta-surface.

Jie Wei received the B.S. and the M.S. degree in School of Physical Science and Technology, Suzhou University of Science and Technology, Suzhou, China. His research interests include the study of microwave biosensors, microwave gas sensors and nanomaterial and MEMS technology in sensing application.

Prof. Dr. Cong Wang was born in 1982, Ph.D. of Engineering, Professor, Doctoral Supervisor, Department of Microwave Engineering, School of Electronics and Information Engineering, Harbin University of Technology. Taking the advantages of semiconductor processing, Prof. Wang has established several research directions with sustainable development potential with the research background of Compound Semiconductor GaAs Passive/GaAs & GaN Active RF, Microwave, Millimeter Wave Devices, Intelligent IoT Sensors and key problems of Disease Diagnosis and Treatment based on Wireless Communication Technology Semiconductor Device Processing and RF Technology and has already made a series of internationally influential achievements in Biomedicine and other cutting-edge directions. It has created a new research direction of RF Microwave Biosensor Design based on ultra-small RF devices, overcome key technical difficulties such as non-reusable RF biosensors, and accelerated the integration of biomedicine, RF technology and Semiconductor Processing.

Kishor Kumar Adhikari received Bachelor in Electronics and Communication Engineering from Tribhuvan University, Institute of Engineering, Nepal, in 2010 and a Doctor in Electronic Engineering from Kwangwoon University, Seoul, Korea in 2016. He was a Postdoctoral Research Associate at Harbin Institute of Technology, Harbin, China from 2017 to 2019. Dr. Adhikari has authored and co-authored over forty journal and international conference papers. His expertise and research interests include the development of high-performance microwave sensors for various applications. To be more precise, his primary research focuses on the synthesis and application of advanced functional nanomaterials and integrating them with micro-fabricated microwave resonators and microfluidics for realizing portable, conformal, and wearable sensors.

Nam-Young Kim was born in 1960 and has received two Masters and two Ph. D. degrees from State University of New York at Buffalo and Midwest University: the M.S. and the Ph. D. in Electronic Engineering. The other degree is M. Div and D.C.E in Theology. He was a research scientist for CEEM at SUNY at Buffalo in 1994. After completing his research at CEEM at SUNY at Buffalo, he joined the Department of Electronic Engineering of Kwangwoon University. He leads the RFIC and RF related Fusion Group at Kwangwoon University, where he has researched along with 12 professors. His research fields are in the areas of RF semiconductor device, RFICs and MMICs, and biosensor applications.